more, if $\dot{\alpha} = 0$, then $\epsilon - \phi = 0$ or π so that $\cos(\epsilon - \phi) = \pm 1$ in Eq. (1). Finally then,

$$\pm I\Omega/I_x p = \cot\alpha - k \csc\alpha \quad \text{at} \quad \dot{\alpha} = \dot{\Omega} = 0$$

that is, $\eta = \pm F(\alpha, k)$ where k is some constant.

It can be seen that $k = \mathbf{H}\cdot\mathbf{u}/I_x p$ $(p \neq 0)$, and, if evaluated prior to entry into an atmosphere, $k = (1 + \eta_0^2)^{1/2} \cos\beta = \cos\beta/\cos\delta$ where β represents the time average angle of attack and δ represents the precessional half cone angle at the high altitudes above the sensible atmosphere. It might be noted from Eq. (5) that, since $C_m < 0$ for an aerodynamically stable body, $\min\Omega$ corresponds to $\max\alpha$ and vice versa. The analysis shows good agreement with six degree of freedom digital program results as shown by Fig. 2. The curves $\eta = +F(\alpha, k)$ associated with large angles of attack are usually the regions of interest.

Though η and thus η_0 are known from body-fixed rate gyro flight data, as a rule, only an estimate of β can be made from a trajectory analysis, thus necessitating a more precise determination of k. To ascertain k for $\eta = +F$, invert this relation to give $(1 + \eta^2) \sin\alpha = -\eta k + \xi$ and $(1 + \eta^2) \cos\alpha = k + \eta\xi$ where $\xi = (1 + \eta^2 - k^2)^{1/2}$.

Consider successive times at which $\dot{\alpha} = \dot{\Omega} = 0$, then

$$(1 + \eta_1^2)(1 + \eta_2^2) \sin\Delta\alpha = k(\xi_2 - \xi_1)(1 + \eta_1\eta_2) - (k^2 + \xi_1\xi_2)(\eta_2 - \eta_1)$$

$$(1 + \eta_1^2)(1 + \eta_2^2) \cos\Delta\alpha = k(\xi_2 - \xi_1)(\eta_2 - \eta_1) + (k^2 + \xi_1\xi_2)(1 + \eta_1\eta_2)$$

Eliminating $k(\xi_2 - \xi_1)$ gives

$$\xi_1\xi_2 = (1 + \eta_1\eta_2) \cos\Delta\alpha - (\eta_2 - \eta_1) \sin\Delta\alpha - k^2$$

Squaring both sides eliminates k^4, and then it can be shown that $k = k^* \sin(\theta - |\Delta\alpha|)$ where

$$k^* = [(1 + \eta_1^2)^{-1} + (1 + \eta_2^2)^{-1} - 2(1 + \eta_1^2)^{-1/2}(1 + \eta_2^2)^{-1/2} \cos(\theta - |\Delta\alpha|)]^{-1/2}$$

and

$$\theta = |\arctan\eta_2 - \arctan\eta_1|$$

From Eqs. (2–4), it can be shown that

$$\Delta\alpha = -\int_{t_1}^{t_2} (q\dot{q} + r\dot{r})[(\dot{q} - \sigma r)^2 + (\dot{r} + \sigma q)^2]^{-1/2} dt$$

An evaluation of the envelope parameter k several times (i.e., for several pair of points where $\dot{\alpha} = \dot{\Omega} = 0$) serves as a check on the data reduction program since k should be a consant for any given flight.

In order to avoid evaluating $\dot{q}$ and $\dot{r}$, the following approximation is proposed:

$$\Delta\alpha \cong -\frac{\Delta\eta}{\lambda - (I/I_x) + 1} \qquad \lambda > I/I_x$$

where

$$\lambda = I(N\pi - \Delta\epsilon)/I_x p\Delta t \qquad N = 0, \pm 1, \pm 2 \ldots$$

and ϵ is determined from Table 1 wherein $\gamma = \arctan|r/q|$, $0 \leq \gamma \leq \pi/2$.

The integer N is chosen on the basis that the computed $\Delta\alpha$ will give a value of k which matches the estimated value given by $k = (1 + \eta_0^2)^{1/2} \cos\beta$ and a trajectory analysis.

The analysis for the case where there is no spin $(p = 0)$ is similar and simpler:

$$\Omega \sin\alpha = [1 + (\Omega_2/\Omega_1)^2 - 2(\Omega_2/\Omega_1) \cos\Delta\alpha]^{-1/2}\Omega_2 \sin|\Delta\alpha|$$

When the angle-of-attack oscillations are fairly well developed, an approximate value of density can be found by integrating Eq. (5), thus

$$\rho_m \cong -I\Delta\Omega^2/AdV^2\Delta G$$

where

$$G = -\int_0^\alpha C_m d\alpha$$

and

$$t_m = (t_1 + t_2)/2$$

Thus, the additional knowledge of velocity, the aerodynamic pitching moment coefficient, and, presumably, altitude is needed.

Table 1 Plane of angle of attack

q	r	ϵ
+	+	$\pi + \gamma$
+	−	$\pi - \gamma$
−	+	$2\pi - \gamma$
−	−	γ

An Experimental Evaluation of Plug Cluster Nozzles

D. Migdal,* J. J. Horgan,† and A. Chamay‡
Pratt and Whitney Aircraft, East Hartford, Conn.

Analysis

If we define the clustered nozzle exit area ratio (ϵ_c) as the circular area enclosing all units divided by the total throat area, and the unit nozzle area ratio (ϵ_N) in the conventional manner, then, for nozzles touching,

$$\epsilon_c/\epsilon_N = (\pi/N + \cos\theta)^2/N$$

where N is the number of units, and θ is the unit nozzle inclination angle.

This simple geometric relationship, combined with well-known isentropic relationships connecting the Prandtl-Meyer angle to the increase in area ratio (from ϵ_N to ϵ_c), is quite helpful in indicating the practical range for a clustered arrangement. For example, a typical rocket motor with $\epsilon_c = 40$ and $\epsilon_N = 7.5$ requires 44 units and a 27° inclination angle if axial flow at ϵ_c is desired. Also, the cluster arrangement is found to be mainly attractive with more than 12 units. With a lower number of units, only a small difference between ϵ_N and ϵ_c is obtained, the individual nozzles are directed almost axially, and the total thrust is essentially the sum of the individual nozzle thrusts.

Test Model and Facilities

All of the data were obtained with high-pressure cold dry air. The plug contours were designed by the axisymmetric method of characteristics assuming annular flow. The individual units were truncated perfect nozzles.[1] The 24-unit model, shown schematically in Fig. 1, was designed with $\epsilon_N = 4$ and $\epsilon_c = 16$. Axial and lateral forces were measured directly

Presented as Preprint 1068-61 at the ARS Solid Propellant Rocket Conference, Salt Lake City, Utah, February 1–3, 1961; revision received March 26, 1964.

* Assistant Project Engineer; presently Senior Gas Dynamics Engineer, Grumman Aircraft, Bethpage, N. Y. Member AIAA.
† Senior Project Engineer.
‡ Assistant Project Engineer. Member AIAA.

and the weight flow computed with a calibrated bell-mouth. A description of the facility is contained in Ref. 2.

Test Results

The ability of a plug nozzle to adjust to various back pressures is well known.[3] A comparison of the off-design characteristics of the cluster and annular plug nozzle is contained in Fig. 2. The performance parameter used (C_V) is the ratio of measured to ideal thrust calculated from the measured weight flow and an isentropic expansion to ambient pressure. The nozzles were tested with several plug lengths obtained by truncating the full-length design contour. As shown in Fig. 3, drastic reductions in plug length have little or no effect on performance.

The effects of spacing between units of the cluster were obtained by blocking the flow through several nozzles to provide symmetric configurations of 12 and 8 operating units. For large gaps between nozzles, the performance loss is appreciable as shown in Fig. 4. The loss is due to the depressurization of the base area between units. A change in plug contour was successful in eliminating this loss.

Results of vectoring by throttling units are shown in Fig. 5. It should be noted that increasing plug length decreases the effectiveness of this type of vectoring. The longer plug acts as a flow diverter, rearranging the initial asymmetric flow back to an almost uniform flow in the axial direction. Note particularly that the side forces actually change sign as the plug length is increased. The results of plug gimballing (Fig. 6) indicate that large angular movements are required to obtain significant side forces. Vectoring by secondary fluid injection normal to the plug surface yielded results similar to injection in a conventional bell nozzle.

Summary and Conclusions

The plug cluster nozzle designed with closely spaced units has performance levels and characteristics identical to the annular plug nozzle. Without modification to the isentropic plug contour, widely spaced units can result in significant thrust losses. Severe truncation of the plug causes little or no loss in performance.

Thrust vector control can be accomplished in several ways. For gimballing or throttling of individual units, the maximum effectiveness is obtained with zero plug length. Shock vector control via secondary injection through the plug wall yielded results equivalent to the same technique in a conventional

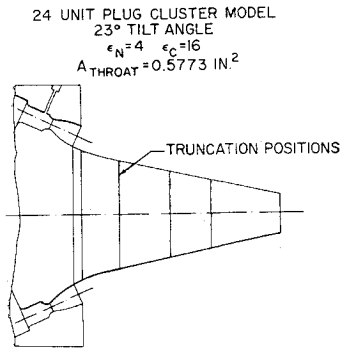

Fig. 1 Plug cluster test model.

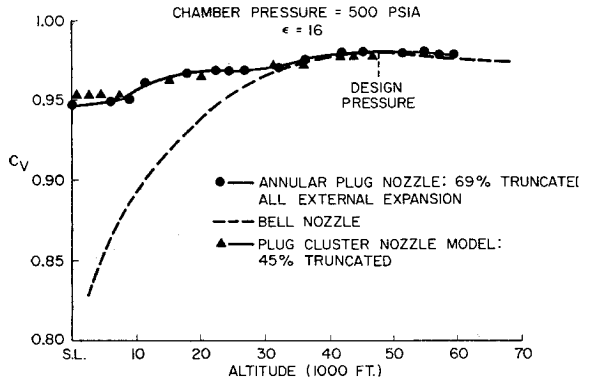

Fig. 2 Off-design characteristics.

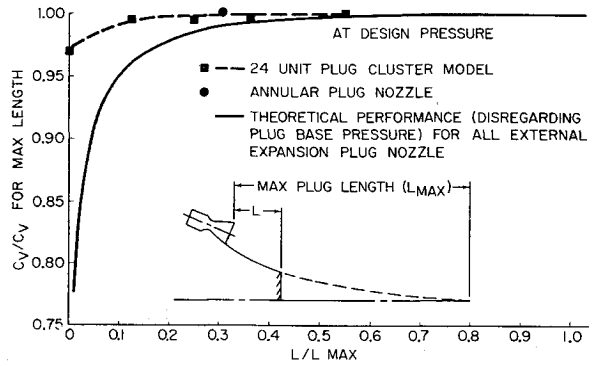

Fig. 3 Effect of plug length.

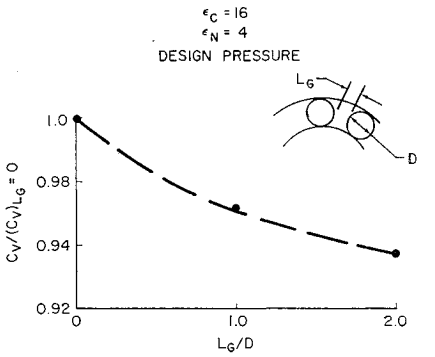

Fig. 4 Effect of gap between nozzles.

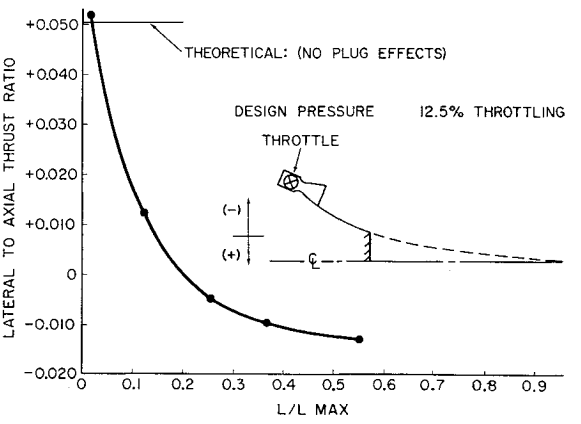

Fig. 5 Throttling individual units.

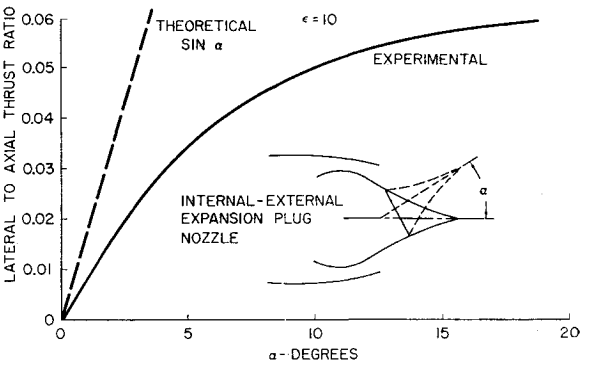

Fig. 6 Plug gimballing.

nozzle. Gimballing a portion of the plug appears to be relatively inefficient, particularly since that portion of the plug which is gimballed can be removed with no decrease in performance. The most promising methods of vectoring appear to be throttling or gimballing the individual nozzles with the shortest plug length consistent with satisfactory unvectored performance.

References

[1] Ahlberg, J. H., Hamilton, S., Migdal, D., and Nilson, E. N., "Truncated perfect nozzles in optimum nozzles design," ARS J. **31**, 614–620 (1961).

[2] Lingen, A., "Jet induced thrust vector control applied to nozzles having large expansion ratios," United Aircraft Corp. RES R-0937-33, East Hartford, Conn. (March 1957).

[3] Berman, K. and Crimp, F. W., Jr., "Performance of plug-type rocket exhaust nozzles," ARS J. **31**, 18–23 (1961).

Falkner-Skan Equation for Wakes

K. Stewartson*
Durham University, Durham City, England

THE existence of physically acceptable solutions of the Falkner-Skan equation

$$f''' + ff'' + \beta(1 - f'^2) = 0 \tag{1}$$

subject to the boundary conditions

$$f(0) = f''(0) = 0 \qquad f'(\infty) = 1 \tag{2}$$

in the range $-\frac{1}{2} \leqslant \beta < 0$ was pointed out by the present author some ten years ago.[1] These solutions have some relevance to the flow in the laminar wake behind a flat-based body, as has been noted by Kennedy,[2] who has also carried out further and more accurate integrations of the equation. From a study of the solutions obtained, he conjectures that as $\beta \to 0-$

$$f' \to f_0' \tag{3}$$

apart from a shift of origin, where f_0 is the solution of (1), with $\beta = 0$, and satisfying

$$f_0'(-\infty) = 0 \qquad f_0'(\infty) = 1 \tag{4}$$

This function has been computed by Chapman.[3]

Further points of interest from the numerical studies[1, 2] are that, if $-0.1988 < \beta < 0$, $f'(0) < 0$, which means that the flow direction in the wake is reversed, and that as $\beta \to 0-$, $f'(0) \to 0-$ having a vertical tangent there. An estimate of the dependence of $f'(0)$ on β near $\beta = 0$ has been given earlier,[1] and in this note an improved version is obtained.

We take (3) as our starting point and show that a consistent solution can be derived from it when β is small. Choose the origin of the independent variable η in (1) so that as $\eta \to -\infty$

$$f_0 = -q + qe^{q\eta} - \frac{q}{4}e^{+2q\eta} + \frac{5q}{72}e^{3q\eta} \ldots \tag{5}$$

where $q = 0.876\ldots$. In consequence, the boundary conditions in (2) are that f and f'' vanish together at some value η^* of η, to be determined. From the numerical integrations, it may be expected that $\eta^* \to -\infty$ as $\beta \to 0-$. The implication of (3) is that, when $|\beta|$ is small and $\eta = O(1)$, we can write

$$f = f_0 + af_1 \tag{6}$$

where a is a small number. Substituting in (1),

$$f_1''' + f_0f_1'' + f_1f_0'' = -(\beta/a)(1 - f'^2) - af_1f_1'' \tag{7}$$

and we now make the further assumption that $|\beta| \ll a$. The right-hand side of (7) is then negligible in the limit $a \to 0$, and the general solution for f_1 is

$$f_1 = Af_0' + B(\eta f_0' + f_0) + C(\eta f_0' + f_0) \times \int_\eta^\infty \frac{f_0'f_0''d\eta}{(2f_0'^2 + f_0'''f_0)^2} - Cf_0' \int_\eta^\infty \frac{f_0''(\eta f_0' + f_0)d\eta}{(2f_0'^2 + f_0'''f_0)^2} \tag{8}$$

where A, B, C are constants. Since $f_1'(\infty) = 0$, $B = 0$, and hence, on substituting the known values of f_0 and integrating, we find that as $\eta \to -\infty$

$$f_1 = (\eta + b)C/q^2 + O(\eta e^{\eta q}) \tag{9}$$

where $b = 1.765/q = 2.014$. Writing $\alpha = -aC/q^2$, it follows that

$$f + \alpha\eta \to -q - \alpha b + O(\alpha^2, \beta) \tag{10}$$

as $\eta \to -\infty$. It is noted that if $\alpha < 0$, $f > 0$ for sufficiently large and negative η. In turn, this implies that f'' ultimately increases exponentially, so that the expansion (5) is not uniformly valid for all η. However, we are only interested in values of $\eta > \eta^*$, at which point f vanishes, but we need to insure that here f'' also vanishes. When $\eta \ll -1$, $f'^2 \ll 1$, and the governing equation takes on the form

$$f''' + ff'' = -\beta \tag{11}$$

We can no longer neglect β, because f'' is exponentially small when $\eta^* < \eta \ll -1$, but this means that to a first approximation we can replace f in (11) by (10), so that (11) becomes

$$f''' - (q + \alpha b + \alpha\eta)f'' = -\beta \tag{12}$$

with solution

$$f'' = D\exp\left[\frac{1}{2\alpha}(\alpha\eta + \alpha b + q)^2\right] - \beta \times \exp\left[-\frac{1}{2\alpha}(\alpha\eta + \alpha b + q)^2\right] \times \int_0^\eta \exp\left[\frac{1}{2\alpha}(\alpha\eta' + q + \alpha b)^2\right]d\eta' \tag{13}$$

Now when $\eta = O(1)$ but large,

$$f''' \approx q^3e^{q\eta} \tag{14}$$

from (5), whence

$$D \doteq q^3\exp\left[-\frac{1}{2\alpha}(q + \alpha b)^2\right] \doteq q^3\exp\left[-\frac{q^2}{2\alpha} - qb\right] \tag{15}$$

Furthermore, using (10), $f = 0$ when

$$\eta = \eta^* \doteq q/\alpha + b \tag{16}$$

and $f'' = 0$ at this point if

$$\beta = -D(2\alpha/\pi)^{1/2} \tag{17}$$

Having obtained an estimate for β in terms of α, the various assumptions made in the course of the argument can now be shown to be consistent. In particular, the neglect of β in (7) and the assumption that the perturbation of f from (10) is negligible even when $\eta = O(\alpha^{-1})$ is justified. We conclude that, when $f = f'' = 0$,

$$f' = -\alpha \tag{18}$$

whence, returning to the origin of η implied in (2), we have that, as $\alpha \to 0+$,

$$\beta \approx -q^3(2\alpha/\pi)^{1/2}\exp[-qb - q^2/2\alpha]$$

where

$$f'(0) \approx -\alpha \tag{19}$$

Received April 27, 1964.

* Professor, Department of Mathematics.